

MECHANICAL AND MICROSTRUCTURAL RESPONSE OF NEAR BETA Ti ALLOYS TO HOT TENSILE TESTING

Hot tensile tests were carried out on Timetal-125 and Timetal-LCB near beta Ti alloys at temperatures in range of 600-1000°C and constant strain rate of 0.1 s⁻¹. At temperatures below 700-800°C, the homogenous and total strains for Timetal-LCB were greater than those for Timetal-125. In contrast, at temperatures over 800°C, Timetal-125 showed better hot ductility. The yield point phenomena was observed in Timetal-LCB at all temperatures. Unlikely, for Timetal-125, it was observed only at temperatures over 800°C. The weaker yield point phenomena in Timetal-125 could be attributed to the negative effect of Al on the diffusion of V. At all temperatures Timetal-LCB exhibited higher strength than Timetal-125. It was found that there should be a direct relationship between the extent of yield point phenomena and strength and dynamic softening through hot tensile testing. It was observed that at temperatures beyond 800°C (beta phase field in both alloys) dynamic recrystallization can progress more in Timetal-125 than in Timetal-LCB. These results were in good agreement with the better hot ductility of Timetal-125 at high temperatures. At low temperatures, i.e. below 700-800°C, partial dynamic recrystallization occurs in beta and dynamic globularization in alpha phase. These processes progress more in Timetal-LCB than in Timetal-125.

Keywords: Thermomechanical processing; Hot deformation; Dynamic softening; Yield point phenomena; Hot ductility

1. Introduction

Beta and near-beta titanium alloys are widely used in automotive, medical and aerospace applications due to their excellent mechanical properties as well as low density [1,2]. Different thermal or thermomechanical treatments in single-phase beta or two-phase alpha+beta regions have been prescribed to develop the desirable mechanical properties in these alloys [3,4].

For most Ti alloys, the initial bulk deformation is carried out in the stability range of beta phase [5,6]. Despite the controversies over the mechanism of dynamic softening in beta [7-11], it has been approved that this phase can afford large deformations and lead to a safe shape change in Ti alloys. However, it is obvious that the chemical composition of beta phase has a strong effect on its mechanical properties and formability at high temperatures. The kinetics of dynamic softening processes, i.e. dynamic recovery (DRV) and dynamic recrystallization (DRX), which play crucial role to the formability, is sensitive to the chemical composition.

The discontinuous yield point is the other important phenomenon which is often observed at low strains during the hot deformation of beta and near-beta alloys. Similar to DRV and DRX, the yield point phenomenon (YPP) depends on chemical composition [12]. The previous works on different alloys have shown that YPP is associated with the immobilization of

dislocations by solute atoms [13-16]. Therefore, the type and content of solute atoms determines the extent of the interaction with dislocations and the extent of YPP. The crucial influence of chemical composition on DRV, DRX and YPP justifies the necessity of acquiring in-dept knowledge about the hot deformation behavior of different beta and near-beta Ti alloys.

Increasing Fe by adding ferroalloys to molten Ti and decreasing other expensive alloying elements such as vanadium is a way to decrease the production cost of titanium alloys. This concept has been the basis for the production of Timetal-LCB (Ti-6.8Mo-4.5Fe-1.5Al) from the original alloy Timetal-125 (Ti-6V-6.2Mo-5.7Fe-2.7Al) [17]. As these alloys are among the most widely used Ti alloys, their mechanical properties and formability at high temperatures are of great importance to the industry. Hence, the present investigation was conducted to analyze the flow behavior and mechanical properties of Timetal-125 and Timetal-LCB through hot tensile testing. The results of this research also help to identify the best regime for the processing of these alloys in the industrial hot working operations.

2. Experimental procedure

The ingots of Timetal-125 and Timetal-LCB, denoted by Ti (125) and Ti (LCB) from this point on, were prepared by melt-

* METALLIC MATERIALS RESEARCH CENTER (MMRC), MALEKE ASHTAR UNIVERSITY OF TECHNOLOGY, TEHRAN, IRAN.

** MATERIALS SCIENCE AND ENGINEERING DEPARTMENT, HAMEDAN UNIVERSITY OF TECHNOLOGY, HAMEDAN, IRAN.

*** MATERIALS SCIENCE AND ENGINEERING DEPARTMENT, SEMNAN UNIVERSITY, SEMNAN, IRAN.

Corresponding author: ammomeni@aut.ac.ir

ing in a vacuum arc remelting (VAR) furnace. Table 1 gives the chemical composition of the alloys. After homogenization and hot rolling at 1150°C, the tensile test samples were prepared in the rolling direction of the rolled specimens according to the ASTM E8M standard. Fig. 1 shows the micrographs of the studied materials before tensile testing. The hot tensile tests were carried out after 3 minutes of soaking at deformation temperatures of 600, 700, 800 and 900°C for Ti (125) and 700, 800, 900 and 1000°C for Ti (LCB). The temperatures have adopted so that one could compare the mechanical properties of alloys in alpha or alpha+beta phase field regions. The beta transus temperatures for Ti (125) and Ti (LCB) have been reported as 700 and 800°C, respectively [17]. All tensile tests were performed to fracture at a constant strain rate of 0.1 s⁻¹. After each test, the broken samples were cooled down to the ambient temperature within 3 seconds and prepared by the standard metallographic techniques (ASTM E3-11) for microstructural observations. After etching in a reagent composed of 2% HF, 10% HNO₃ and 88% distilled water, the prepared samples were examined using an optical microscope model Olympus-BXSL.

TABLE 1

Chemical compositions of Ti (125) and Ti (LCB) used in this investigation (all in wt.%)

Alloy	V	Al	Fe	Mo	Ti
Ti (125)	6.01	2.74	5.71	6.03	Rem.
Ti (LCB)	0.02	1.51	4.51	6.82	Rem.

3. Results and discussion

3.1. Flow curve analysis

The true stress-strain curves of the materials, calculated from the load-stroke data, are shown in Fig. 2. Both alloys clearly show more formability with an increase in temperature. However, some differences were observed in strength levels, total strain and the flow behaviors which should be addressed in detail. The flow behaviors of the materials can be divided into some similar steps. The steps can be identified by superimposing the work hardening rate curve on the stress-strain curve, typically shown

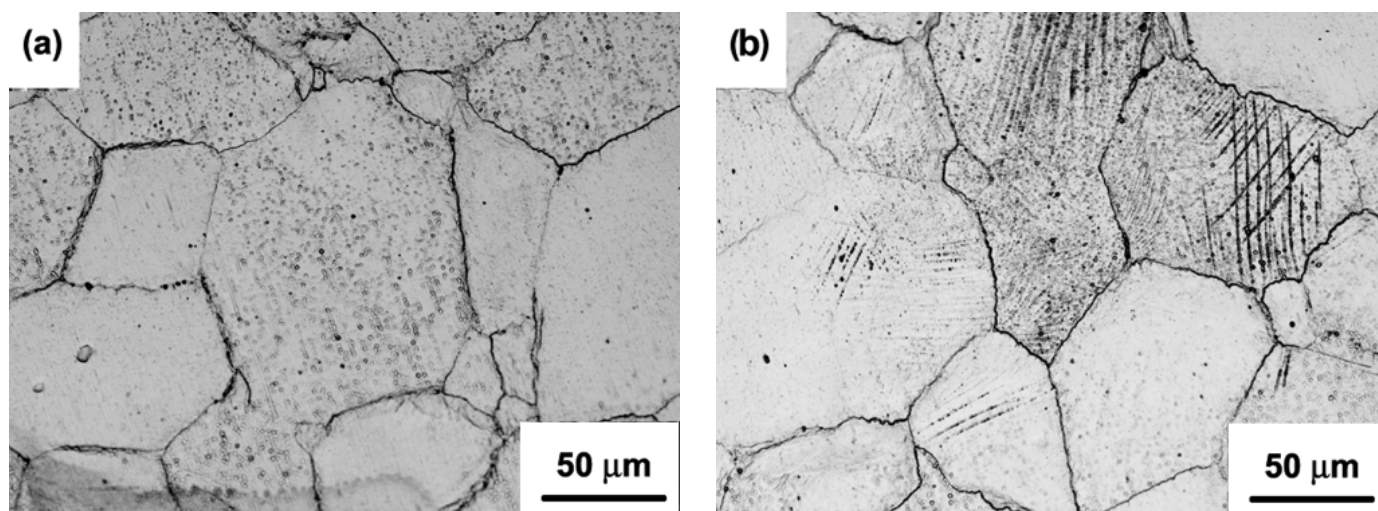


Fig. 1. Starting microstructures of the studied materials: (a) Ti (125), (b) Ti (LCB)

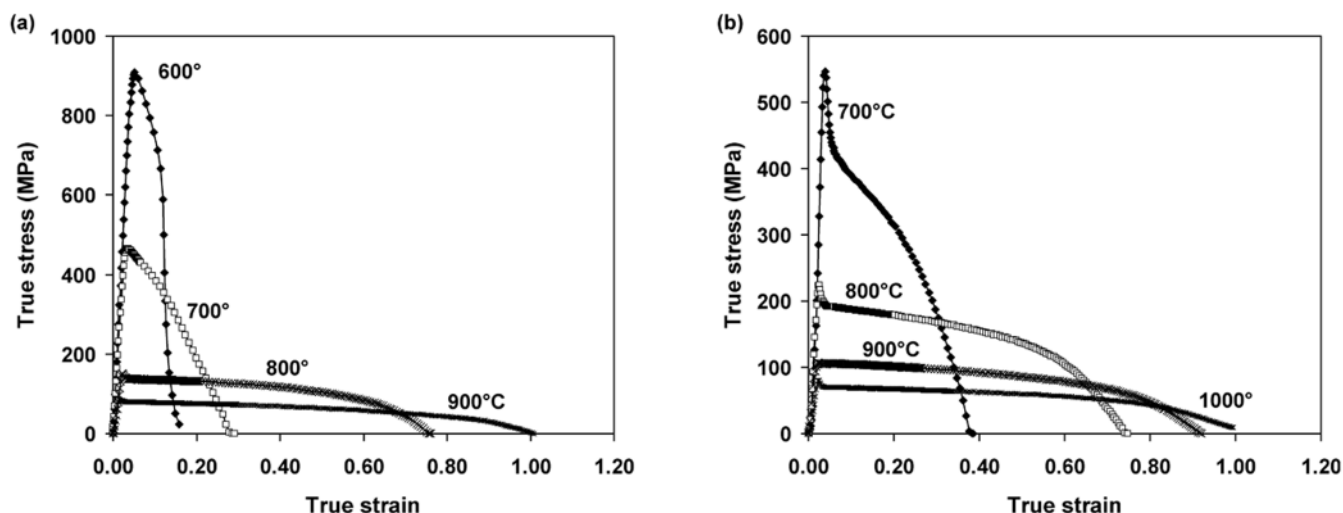


Fig. 2. True stress-strain curves of the studied alloys at different temperatures and strain rate of 0.1 s⁻¹: (a) Ti (125), (b) Ti (LCB)

for both alloys at 900°C in Fig. 3. As it is observed, the flow curves are comprised of three distinct regions. These regions can be distinguished by the variation of ds/de with strain. The first region for both alloys shows the elastic behavior, yield point and the early stages of plastic deformation. This region, which may contain YPP, depending on the alloy and temperature, ends up reaching a peak stress and is followed by a relatively gradual flow softening in region II. At some temperatures (800 and 900°C for Ti (125) and all temperatures for Ti (LCB)) the flow curves show YPP between regions I and II. The decreasing $d\sigma/d\varepsilon$ in region II suggests that dynamic softening processes, DRV or DRX, dominate the flow behavior. In region III, the rate of flow softening increases considerably and the flow stress decreases abruptly down to zero at breaking. In this region, the flow softening occurs geometrically due to necking. It is then followed by dimples initiation and propagation and finalized by breaking. Hence, the border between regions II and III can be introduced as the start of plastic anisotropy in the necked samples. It is therefore possible to consider regions II and III as the homogeneous and inhomogeneous deformation regimes, respectively.

3.2. Flow softening and ductility at high temperatures

The sectioning method presented in Fig. 3 helps to quantify the potential of dynamic softening and plastic instability in the materials by comparing the lengths of corresponding regions at different temperatures. Fig. 4 shows the lengths of regions II and III (homogeneous and necking strains) and the total strain to fracture as the functions of tensile temperature. It is observed that the homogeneous and total strains for Ti (125) are larger than those for Ti (LCB) at high temperatures, i.e. over 800°C. However, at temperatures below 800°C, the condition is overturned. The necking strain of Ti (125) is larger than that of Ti (LCB) over the whole studied temperature range. These results implicitly indicate that Ti (125) and Ti (LCB) have greater tendencies for dynamic softening respectively at high and low temperatures. It is to be added that with regard to the beta transus temperatures, 700°C for Ti (125) and 800°C for Ti (LCB) [17], at temperatures over 800°C, both alloys have a single-phase beta microstructure. The undulating trend of necking strain-temperature curves seems to be due to the transition from two-phase (alpha+beta) to sin-

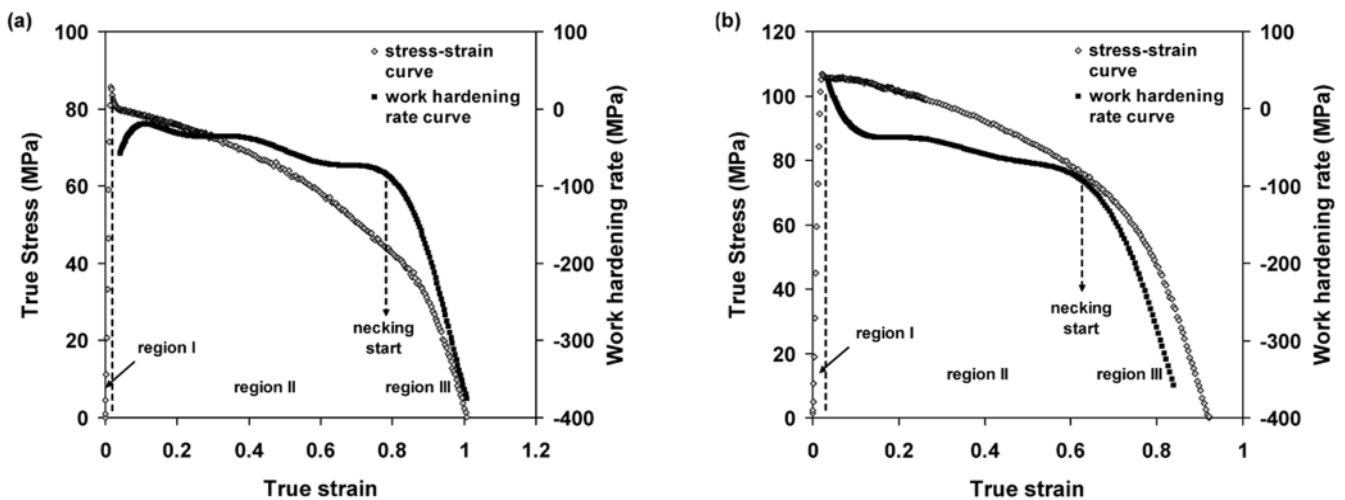


Fig. 3. Typical work hardening curves for the studied alloys, (a) Ti (125), (b) Ti (LCB), at 900°C, superimposed on the corresponding stress-strain curves. The regions of elastic behavior and yielding, flow softening and necking are characterized by notations I, II and III

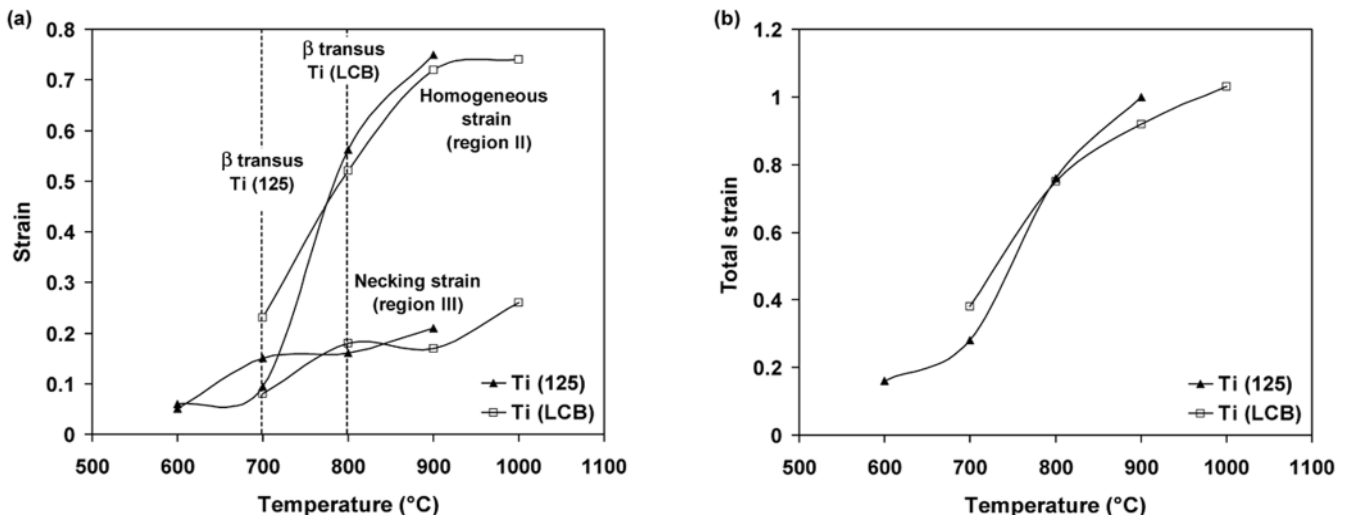


Fig. 4. Variation of (a) homogeneous and necking strains and (b) total strain to fracture for the studied materials

gle phase (beta) region. The inflection points of the curves are consistent with the beta transus temperatures of 700 and 800°C for Ti (125) and Ti (LCB) alloys, respectively.

Having a large stacking fault energy (SFE), beta phase has been found prone to undergo extensive DRV and sluggish continuous DRX (CDRX) during hot working [6,18,19]. Hence, increasing alloying elements to beta phase can change the mechanism of dynamic softening to the conventional discontinuous DRX (DDRDX), if they effectively decrease SFE. Few released publications over the topic have shown that Al and V tend to decrease SFE in Ti [20,21]. Therefore, the higher ductility of Ti (125), in comparison to Ti (LCB), at high temperatures can be associated with the addition of 6 wt. % V, 1 wt. % Fe and 1 wt. % Al, which might increase the tendency for faster DRX and postpone flow localization and final fracture.

3.3. Flow softening and ductility at low temperatures

At low temperatures, i.e. below 700-800°C, both alloys are duplex alpha+beta. Hence, DRX in beta phase is not the only softening mechanism as is at high temperature ranges. The results presented in Fig. 4 show that low temperature range, dynamic softening is faster in Ti (LCB) than in Ti (125), justifying the better ductility in the former alloy. In addition, it is interesting that the results indicate a relationship between ductility and YPP. In order to show a better observation over the yield points, the magnified view of the flow curves has been provided in Fig. 5. The variation of upper and lower yield stresses (σ_U and σ_L) and the yield drop ($\sigma_U - \sigma_L$) with tensile temperature has been represented in Fig. 6. Unlike to Ti (LCB), the flow curves of Ti (125) do not show YPP at temperatures below 700°C. It seems that there should be a relationship between the absence of YPP and low total strains in Ti (125). The lower tendency for YPP in Ti (125) is in contrast to the results of literature on the role of vanadium in pinning dislocations and causing YPP [18]. This paradox can be resolved by considering the interactions between

alloying elements. For example, Takahashi et al [22] showed that Al can decrease the diffusion of V in beta Ti alloys. The faster diffusion of Al in Ti, which is due to its smaller atomic radius (125 pm), decreases the diffusivity of larger atoms such as V ($r = 135$ pm), Mo ($r = 145$ pm) and Fe ($r = 140$ pm) and even self Ti ($r = 140$ pm). Therefore, weak YPP in Ti (125) can be attributed to the existence of large amount of Al in this alloy. The results imply that YPP has a positive effect on the dynamic softening and gives rise to increasing total strain in Ti (LCB). It seems that pinning the primary dislocations through YPP boosts the production of new dislocations at the earlier stages of yielding. Therefore, for a material which shows YPP during yielding, a larger dislocation density than usual will be available for the next steps of deformation. This in turn increases the tendency for dynamic softening which renders better formability and more resistance to plastic instability and fracture. Fig. 7 summarizes the effect of tensile temperature on the mechanical properties of the studied materials. It is observed that at low temperatures; due to the effect of YPP, the upper yield stress (σ_U) for Ti (LCB) is about 33% larger than that of Ti (125). However, at high temperatures, i.e. beyond 800°C, the difference decreases to about 25%. As a conclusion, all the results in Figs. 4,6 and 7 show that Ti (125) and Ti (LCB) represent better ductility at high and low temperatures, i.e. below and beyond 800°C, respectively.

3.4. Microstructures at high temperatures

As it was discussed in Figs. 4-7, Ti (125) represents better ductility with respect to Ti (LCB), especially at temperature beyond 800°C. It was attributed to the easier DRX in Ti (125) comparing to Ti (LCB). In order to verify the results presented in the previous section, the optical micrographs of the deformed samples are compared in Fig. 8. At 800 and 900°C the micrographs presented in Figs. 8a and 8c for Ti (125) are characterized by large DRX grains with regular grain boundaries. However, those for Ti (LCB) at the same temperatures in Figs. 8b and

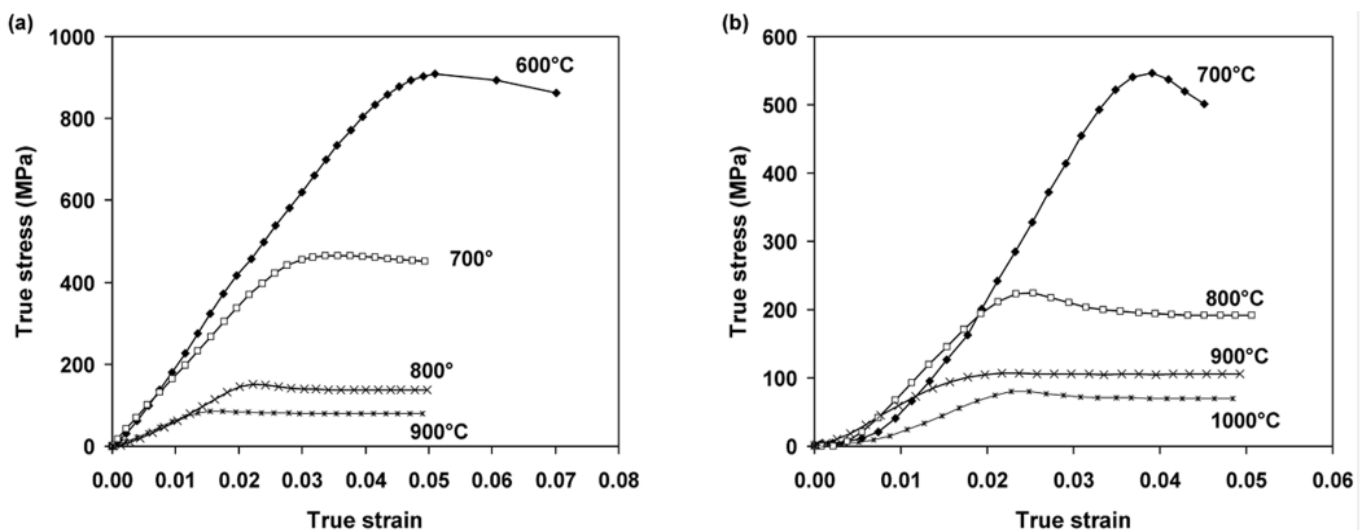


Fig. 5. Magnifies view of the flow curves showing the yield point phenomenon for: (a) Ti (125), (b) Ti (LCB)

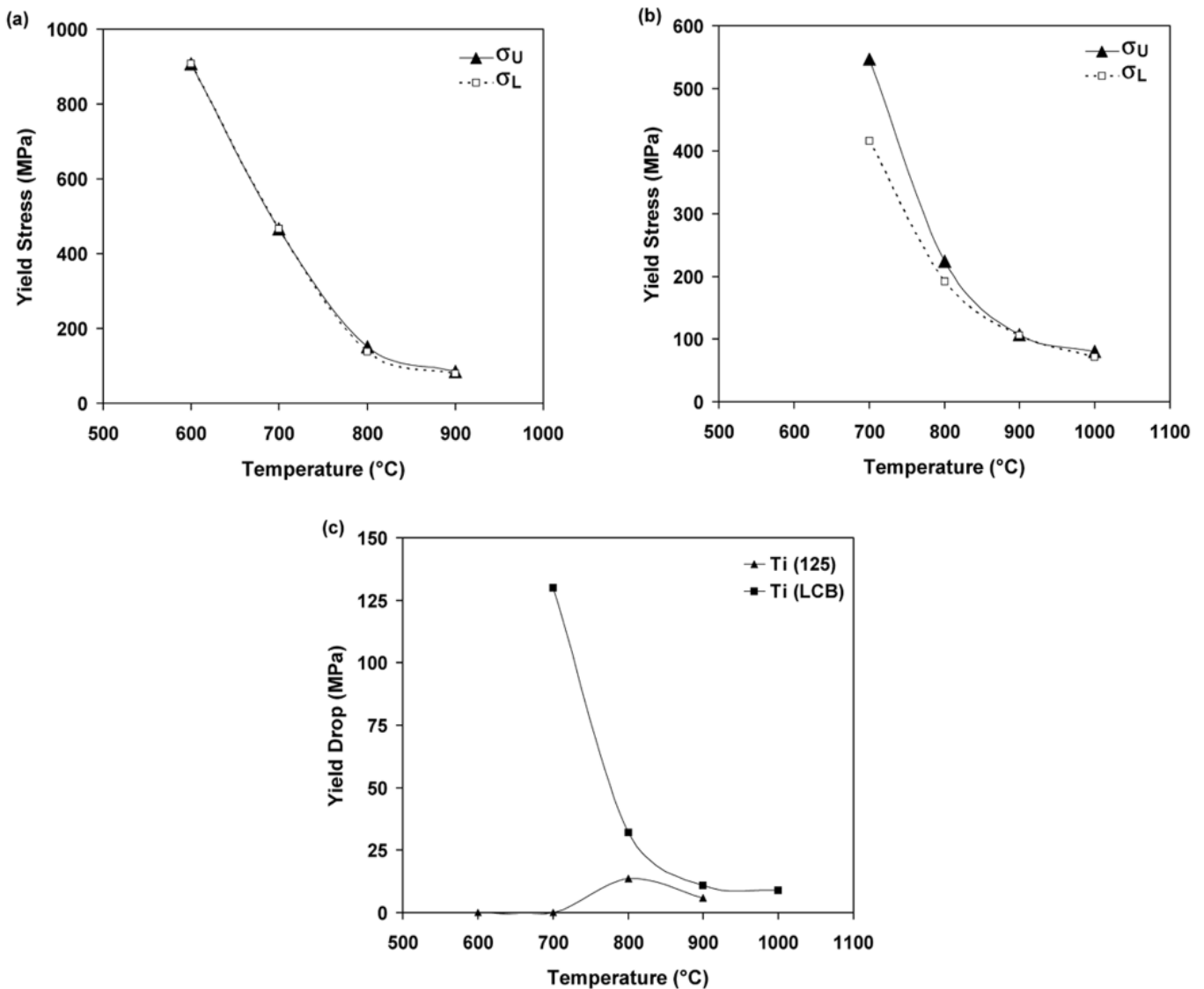


Fig. 6. Variation of the upper and lower yield stresses (σ_U and σ_L) with tensile temperature for (a) Ti (125), (b) Ti (LCB), and (c) variation of yield drop for both alloys with temperature

8d show serrated grain boundaries, which are typical of partial DRX. It should be noted that the grain boundary serration is a response to the tension exerted by the sub-boundaries which are well-developed during extended DRV. It has been reported in the literature that in beta Ti alloys the grain boundary serration happens due to CDRX which progresses with the gradual change of sub-grains to the DRX grains [18]. By increasing temperature to 1000°C, Fig. 8e, the rate of DRV and CDRX increases and leads to the formation of DRX grains with regular grain boundaries.

3.5. Microstructures at low temperatures

The micrographs of the hot deformed samples at 600 and 700°C are shown in Fig. 9. For Ti (LCB), the micrographs presented in Figs. 9a and 9b respectively indicate the microstructural evolutions in beta and alpha phases at two different magnifica-

tions. The serrated grain boundaries which are observed in Fig. 9a implied that beta phase has undergone partial DRX. In addition, the magnified view of microstructure in Fig. 9b indicates the considerable globularization of alpha phase particles, especially adjacent the beta grain boundaries. These observations comply with the mechanical testing results and confirm that the dynamic softening mechanisms in both phases are the reason for good ductility of Ti (LCB) at low temperatures. On the other hand, the microstructures of Ti (125) at 700°C, shown in Figs. 9c and 9d, exhibit slightly serrated grain boundaries in beta and partial globularization of alpha phase particles. At the same condition the less progress of DRX and dynamic globularization in Ti (125) is the reason for its lower ductility and total strain, comparing to Ti (LCB). Figs. 9e and 9f confirm that by decreasing temperature to 600°C, DRX in beta and dynamic globularization in alpha phase degrades and the lamellar structure of alpha+beta remains nearly intact. This leads to more degradation of ductility that is evident from the mechanical results in Figs. 4 and 7.

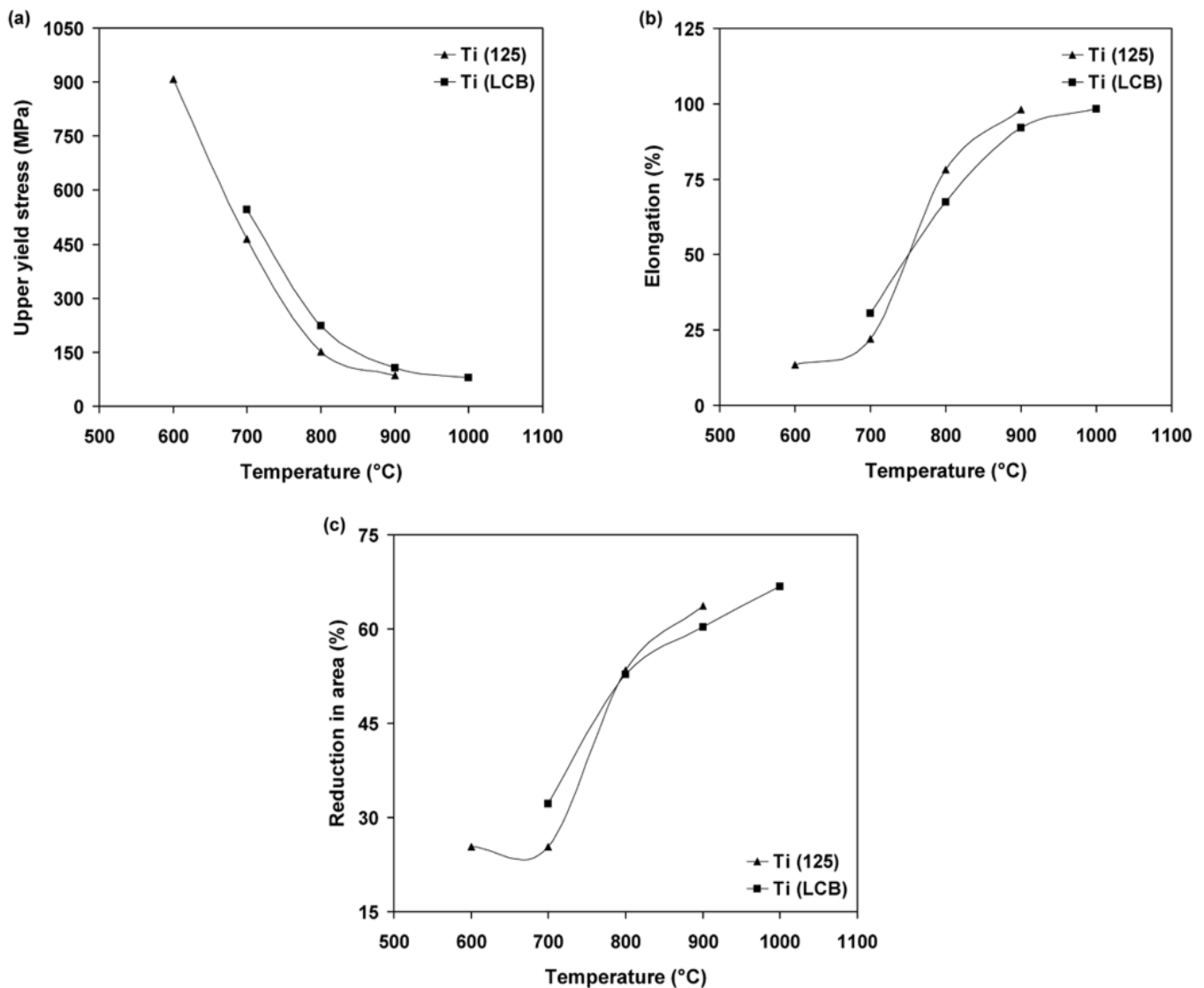


Fig. 7. Variation of (a) the upper yield stress, (b) total elongation and (c) reduction in area with tensile temperature, for both alloys

4. Conclusions

Hot tensile tests were carried out on Ti (125) and Ti (LCB) near beta alloys at temperatures in range of 600-1000°C. The major results of this research can be summarized as follows:

- At temperatures below 700-800°C, the homogenous and total strains for Ti (LCB) were greater than those for Ti (125). The elongation and reduction in area confirmed the same finding.
- At temperatures over 800°C, Ti (125) showed better ductility and higher elongation and reduction in area.
- The yield point phenomena was observed in Ti (LCB) at all temperatures. However, for Ti (125), it was traceable only at temperatures over 800°C. The weaker yield point phenomena in Ti (125) was attributed to the negative effect of Al on the diffusion of V.
- At all temperatures Ti (LCB) exhibited higher strength than Ti (125). It was because the yield point phenomena was more considerable in the former alloy.
- It was found that there is a direct relationship between the extent of yield point phenomena (yield drop) and dynamic softening through hot tensile testing. It is suggested that the multiplication of dislocations during the early stages of yielding stimulates dynamic softening through the latter deformation.
- It was observed that at temperatures beyond 800°C (beta phase field in both alloys) dynamic recrystallization can progress more in Ti (125) than in Ti (LCB). These results were in good agreement with the better hot ductility of Ti (125) at high temperatures.
- At low temperatures, i.e. below 700-800°C, dynamic softening was comprised of partial dynamic recrystallization in beta and dynamic globularization in alpha phase. The processes were more rapidly in Ti (LCB) than in Ti (125).

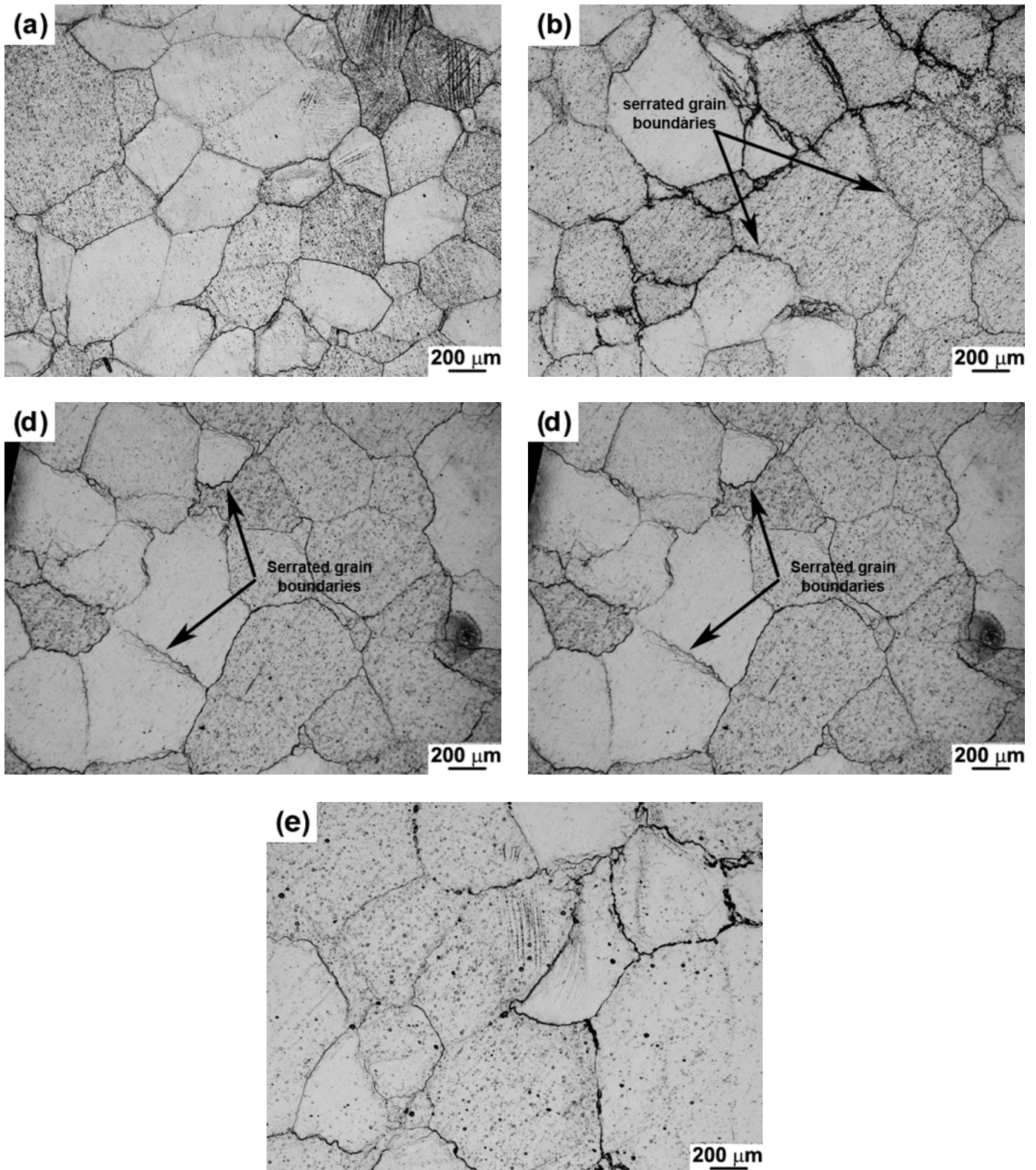


Fig. 8. Microstructures of the deformed specimens at high temperatures: (a) Ti (125), 800°C, (b) Ti (LCB), 800°C, (c) Ti (125), 900°C, (d) Ti (LCB), 900°C, (e) Ti (LCB), 1000°C

REFERENCES

- [1] J. Klimas, A. Łukaszewicz, M. Szota, M. Nabialek, *Arch Metall Mater* 60, 2013-2018 (2015).
- [2] O.M. Ivasishin, P.E. Markovsky, Yu.V. Matviychuk, S.L. Semiatin, C.H. Ward, S. Fox, *J. Alloys Comp.* **457**, 296-309 (2008).
- [3] S.M. Abbasi, A. Momeni, *Trans. Nonferrous Met. Soc. Chin.* 21, 1728-1734 (2011).
- [4] R. Bogucki, K. Mosór, M. Nykiel, *Arch. Metall. Mater.* 59, 269-1273 (2014).
- [5] V.V. Balasubrahmanyam, Y.V.R.K. Prasad, *J. Mater. Eng. Perform.* 10, 731-739 (2001).

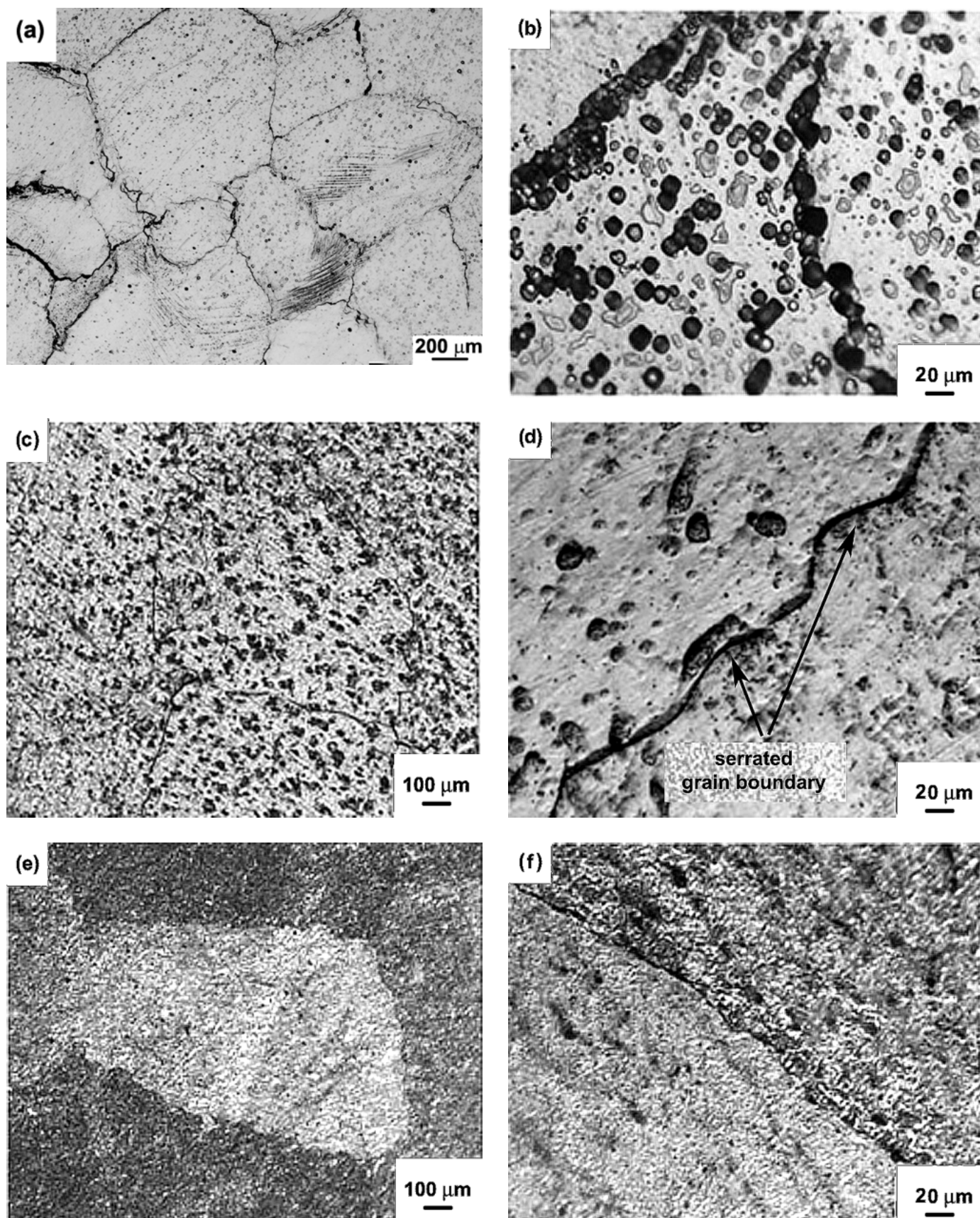


Fig. 9. Microstructures of the deformed specimens at low temperatures: (a) Ti (LCB), 700°C, (b) magnified view of (a), (c) Ti (125), 700°C, (d) magnified view of (c), (e) Ti (125), 600°C, (f) magnified view of (e)

- [6] S.M. Abbasi, A. Momeni, A. Akhondzadeh, S.M. Ghazi Mirsaed, *Mater. Sci. Eng.* **A639**, 21-28 (2015).
- [7] J.K. Fan, H.C. Kou, M.J. Lai, B. Tang, H. Chang, J.S. Li, *Mater. Sci. Eng.* **A584**, 121-132 (2013).
- [8] H. Matsumoto, L. Bin, S.H. Lee, Y. Li, Y. Ono, A. Chiba, *Met. Mater. Trans.* **44A**, 3245-3260 (2013).
- [9] A.H. Sheikhal, M. Morakkabati, S.M. Abbasi, A. Rezaei, *Int. J. Mater. Research* **104**, 1122-1127 (2013).
- [10] M. Kukuryk, *Arch. Metall. Mater.* **60**, 1639-1647 (2015).
- [11] A. Momeni, S.M. Abbasi, *Mate. Design* **31**, 3599-3604 (2010).
- [12] A. Momeni, S.M. Abbasi, M. Morakabati, A. Akhondzadeh, *Mater. Sci. Eng.* **A643**, 142-148 (2015).
- [13] I. Philippart, H.J. Rack, *Mater. Sci. Eng.* **A243**, 196-200 (1998).
- [14] V.V. Balasubrahmanyam, Y.V.R.K. Prasad, *Mater. Sci. Eng.* **A336**, 150-158 (2002).
- [15] B.M. Hance, *J. Mater. Eng. Perform.* **14**, 616-622 (2005).
- [16] Z. Li, L. Fu, B. Fu, A. Shan, *Mater. Lett.* **96**, 1-4 (2013).
- [17] P.G. Allen, A.J. Hull, *Proceeding of the 1994 International Titanium Conference*, Titanium Development Association, 397 (1994).
- [18] S.M. Abbasi, M. Morakabati, A.H. Sheikhal, A. Momeni, *Met Mater Trans* **45A**, 5201-5211 (2014).
- [19] T. Chandra, M. Ionescu, D. Mantovani, *Mater. Sci. Forum* **706-709**, 127-134 (2012).
- [20] Z. Guo, A.P. Miodownik, N. Saunders, J.Ph. Schillé, *Scripta Mater.* **54**, 2175-2178 (2006).
- [21] C. Leyens, M. Peters (Eds.), *Titanium and titanium alloys: fundamentals and applications*, 2003 Wiley-VCH.
- [22] T. Takahashi, Y. Minamino, M. Komatsu, *Mater. Trans.* **49**, 125-132 (2008).